Published in final edited form as:
Radiat Res. 2009 November ; 172(5): 592–597. doi:10.1667/RR1781.1.

Radiotherapy in Conjunction with 7-Hydroxystaurosporine: A Multimodal Approach with Tumor pO_2 as a Potential Marker of Therapeutic Response

Nadeem Khan[a,b,1], **Sriram P. Mupparaju**[a], **Huagang Hou**[a,b], **Jean P. Lariviere**[a], **Eugene Demidenko**[b], **Harold M. Swartz**[a,b], and **Alan Eastman**[b]

[a]EPR Center for Viable Systems, Dartmouth Medical School, Hanover, New Hampshire 03755

[b]Norris Cotton Cancer Center, Dartmouth-Hitchcock Medical Center, Lebanon, New Hampshire 03756

Abstract

Checkpoint inhibitors potentially could be used to enhance cell killing by DNA-targeted therapeutic modalities such as radiotherapy. UCN-01 (7-hydroxystaurosporine) inhibits S and G_2 checkpoint arrest in the cells of various malignant cell lines and has been investigated in combination with chemotherapy. However, little is known about its potential use in combination with radiotherapy. We report the effect of 20 Gy radiation given in conjunction with UCN-01 on the pO_2 and growth of subcutaneous RIF-1 tumors. Multisite EPR oximetry was used for repeated, non-invasive tumor pO_2 measurements. The effect of UCN-01 and/or 20 Gy on tumor pO_2 and tumor volume was investigated to determine therapeutic outcomes. Untreated RIF-1 tumors were hypoxic with a tissue pO_2 of 5–7 mmHg. Treatment with 20 Gy or UCN-01 significantly reduced tumor growth, and a modest increase in tumor pO_2 was observed in tumors treated with 20 Gy. However, irradiation with 20 Gy 12 h after UCN-01 treatment resulted in a significant inhibition of tumor growth and a significant increase in tumor pO_2 to 16–28 mmHg from day 1 onward compared to the control, UCN-01 or 20-Gy groups. Treatment with UCN-01 12 h after 20 Gy also led to a similar growth inhibition of the tumors and a similar increase in tumor pO_2. The changes in tumor pO_2 observed after the treatment correlated inversely with the tumor volume in the groups receiving UCN-01 with 20 Gy. This multimodal approach could be used to enhance the outcome of radiotherapy. Furthermore, tumor pO_2 could be a potential marker of therapeutic response.

INTRODUCTION

In spite of recent developments in dose delivery for radiotherapy (1), tumor hypoxia continues to be a major limiting factor in therapeutic success (2–4). The tumor tissue pO_2 (partial pressure of oxygen) is strongly correlated with the prognosis: the more hypoxic the tumor, the worse the prognosis, in terms of both local control with radiotherapy and the appearance of distant metastases (4,5). Tumor hypoxia also promotes more aggressive tumor behaviors (4). This warrants new approaches to enhance the outcome of radiotherapy. With the increased use of radiotherapy in combination with chemotherapy or after surgery for the treatment of various malignancies, the changes in tumor pO_2 and consequent possible effects on the outcomes also should be considered.

[1]Address for correspondence: EPR Center for Viable Systems, 703 Vail, Dartmouth Medical School, Hanover, NH 03755; Nadeem.khan@dartmouth.edu.

Until recently, the lack of a suitable method for repeated tumor pO_2 measurements during therapy has been a limiting factor in optimization of radiotherapy based on tumor pO_2. Electron paramagnetic resonance (EPR) oximetry is a relatively new method based on the sensitivity of implanted paramagnetic material to the local oxygen content and allows repeated non-invasive (after the placement of the paramagnetic material) measurements of tissue pO_2 from the same sites in the animals over long periods (6,7). Using this technique, we have reported tumor growth delay in experimental tumors when irradiated at times of higher pO_2 compared to when the tumors were hypoxic (8–10). This technique has also been used to determine the effect of hypoxia modifiers on tumor oxygenation and radiotherapeutic outcome (9,11,12). The recent development of multisite EPR oximetry has allowed simultaneous pO_2 measurements at several sites in a tissue of interest (10,12). At present, this technique is being investigated for its clinical feasibility in patients with tumors within 10 mm from the surface (7,13). The ability to follow the time course of tumor pO_2 over the course of therapy, such as by EPR oximetry, could provide the crucial information needed to optimize radiotherapy and the effectiveness of hypoxia-modifying procedures. Such information could be used to individualize the clinical use of fractionated radiotherapy and multimodality treatments.

Cell cycle arrest in response to radiation-induced DNA damage further compromises the radiotherapeutic outcome. The cell cycle checkpoints are complex signal transduction networks that integrate the cellular responses to DNA insults by arresting cell cycle progression to facilitate DNA repair (14). Consequently, checkpoint inhibitors are being considered as potential molecular manipulations to enhance the effect of DNA-damaging therapies and thereby augment outcome by driving the malignant cells through the cell cycle, resulting in lethal mitosis. Among these, UCN-01 (7-hydroxystaurosporine) was discovered by Eastman *et al.* to inhibit S and G_2 checkpoint arrest in various malignant cell lines (15–17). UCN-01 inhibits Chk1 and has been investigated extensively in combination with chemotherapy (15, 18–21). However, little is known about its possible *in vivo* efficacy in conjunction with radiotherapy. To our knowledge, the only report is by Tsuchida *et al.*, who investigated the effect of UCN-01 combined with fractionated radiotherapy (10 Gy × 7) in experimental FSA-II tumors (22). The synergistic effect of UCN-01 in combination with radiotherapy is suggested to be due to inhibition of clonogenic repopulation and the accumulation of the cells in the radiosensitive G_2/M phase. The effects of the timing of the UCN-01 and radiotherapy on the therapeutic outcome and the changes in tumor pO_2 during this multimodal treatment are not known. This information would be potentially useful to establish a rational approach for efficiently combining these two modalities and might also provide a potential marker to predict outcome. We therefore have investigated the effect of radiotherapy (20Gy) and/or UCN-01 on tissue pO_2 and growth of experimental subcutaneous RIF-1 tumors. The tumors were treated with UCN-01 either 12 h before or after irradiation to investigate the effect of UCN-01 schedule on therapeutic outcome and tumor pO_2.

MATERIALS AND METHODS

Animals and Tumor Models

All animal care and use protocols were approved by the Institutional Animal Care and Use Committee (IACUC) of Dartmouth Medical School. The radiation-induced fibrosarcoma tumor (RIF-1) cells were obtained from Dr. J. B. Mitchell's laboratory at the National Cancer Institute. The RIF-1 cells were cultured in RPMI 1640 medium supplemented with 10% FBS, glutamine and antibiotics. For tumor inoculation, female C3H/HEJ mice weighing 18–20 g (Charles River Laboratories, Wilmington, MA) were anesthetized using 1.5% isoflurane with 30% FiO_2 (fraction of inspired oxygen), and a suspension of 5×10^5 cells in 50 μl FBS-free medium was injected subcutaneously into the left posterior flank of each mouse.

Paramagnetic Probe Insertion for EPR Oximetry

The tumors were allowed to grow for 12–15 days after cell inoculation to reach a tumor diameter of approximately 6–8 mm. Then we injected two aggregates of the oxygen-sensitive lithium phthalocyanine (LiPc, paramagnetic oximetry probe) crystals for pO_2 measurements at two sites in each tumor by EPR oximetry (multisite EPR oximetry).

LiPc crystals were synthesized in our laboratory; their physicochemical properties and application for pO_2 measurements have been described previously (7,9,12,23). Briefly, the EPR spectra of LiPc crystals exhibit a single sharp EPR line with a line width that is highly sensitive to pO_2 and reflects the average pO_2 on the surface of the crystals. The high density of the unpaired spins along with the narrow intrinsic line width of LiPc allows measurements of pO_2 in the tumor tissue using few crystals with a total diameter of ~200 μm.

The mice were anesthetized, and two aggregates of the LiPc crystals (30–50 μg each) were inserted into each tumor using 25-gauge needles. The depth of the LiPc implants was about 2 mm from the tumor surface, and the distance between the two implants was approximately 4–5 mm. The experiments were started 24 h after LiPc insertion (day 0).

UCN-01

UCN-01 was generously provided by Dr. Edward Sausville (National Cancer Institute, Bethesda, MD). The UCN-01 was dissolved in 0.1 *M* sodium acetate (pH 5) to obtain a solution of 3.75 mg UCN-01/ml. Alzet osmotic pumps (Model 1003D, DURECT Corporation, Cupertino, CA) were loaded with UCN-01 solution (90 μl) and implanted subcutaneously on the back of each mouse using the procedures recommended by DURECT. These osmotic pumps allowed systemic administration of 1 μl of UCN-01 per hour of infusion for 3 consecutive days. The pumps were removed on day 4. The dose administered was based on preliminary experiments that predicted a plasma concentration of 100 n*M* with this dose regimen.

Measurement of UCN-01 Concentration in the Plasma

The mice were chosen randomly and blood samples were collected at 24 and 48 h. The plasma was separated by microcentrifugation at 10,000 rpm for 10 s and stored at −70°C for analysis. The plasma concentration of the UCN-01 was determined using high-performance liquid chromatography (17). Briefly, the detection of UV absorbance was set at 295 nm for UCN-01 and 323 nm for umbelliferone (internal standard). The coefficient of determination (r^2) for the UCN-01 plasma concentration calibration curves was 0.99, and the lower limit of detection was 0.5 μg/ml.

Electron Paramagnetic Resonance (EPR) Oximetry

EPR oximetry measurements were performed on an L-band (1.2 GHz) EPR spectrometer equipped with a microwave bridge and an external loop resonator specially designed for *in vivo* experiments (6,24). The two LiPc implants in each tumor were located along the lateral axis. For multisite EPR measurements, the animals were positioned in the spectrometer such that this axis was parallel to the direction of the applied gradient in the main magnetic field. A gradient of up to 3.0 G/cm was used to separate the EPR signals of the two LiPc implants in each tumor (9,23). The spectrometer parameters for the EPR acquisition were: incident microwave power, 2 mW; magnetic-field center, 425 gauss; scan range, 1.5 gauss; modulation frequency, 27 kHz; modulation amplitude less than one-third of the EPR line width; scan time of 10 s. We averaged 11 scans each to enhance the signal-to-noise ratio of the EPR signals. The EPR line widths were converted to pO_2 using a calibration plot determined for the batch of LiPc crystals used in this study. No significant difference in the pO_2 obtained from the two

LiPc implants in each tumor was observed, and the values were pooled to obtain average tumor pO_2.

Irradiation

For irradiation of the tumors, the animals were anesthetized and moved to the irradiator bed of a Varian Clinac 2100C Linear Accelerator (energy: 6 MeV; applicator: 6 cm × 6 cm). The beam was focused on the tumor, and appropriate lead shields were used to prevent irradiation of the normal tissue. The animals were returned back to the animal facility after irradiation.

Experiment Protocol

Mice were assigned randomly to one of the five groups: (1) control, $n = 8$, (2) 20 Gy alone, $n = 7$, (3) UCN-01 alone, $n = 8$, (4) UCN-01 (time 0) + 20 Gy (12 h), $n = 8$, and (5) 20 Gy (time 0) + UCN-01 (12 h), $n = 6$.

Groups (4) and (5) are referred to as UCN-01/20 Gy and 20 Gy/UCN-01, respectively, throughout this paper. These groups were used to investigate the effect of UCN-01 sequence on tumor pO_2 and growth. For tumor pO_2 measurements, the mice were anesthetized (1.5% isoflurane, 30% FiO_2) and positioned in the EPR magnet. A warm air blower and a heated water pad were used to keep the animal warm. The rectal temperature of the animal was monitored and maintained at 37 ± 0.5°C during the measurements. The tumor pO_2 was measured for 25 min each day for 6 consecutive days (day 0–day 5) using multisite EPR oximetry. The osmotic pumps were implanted in the mice of groups (3) and (4) on day 0 (i.e. time 0) after baseline pO_2 measurements. Approximately 12 h later, the tumors of group (4) were irradiated with 20 Gy; tumor pO_2 was measured each day thereafter for 5 successive days. A similar protocol was followed for group (3), but the tumors were not irradiated. The tumors of group (5) were irradiated on day 0 and the pumps were implanted 12 h later for UCN-01 treatment; the measurements were continued as described for the other groups. The tumor was measured each day prior to pO_2 measurements and the volume was calculated by a standard procedure (volume = $\pi/6 \times \text{length} \times \text{width}^2$) for 7 consecutive days. The tumor pO_2 and volume measured on day 0 prior to any treatment are regarded as the baseline values.

Statistical Analysis

A paired *t* test was used to determine the statistical significance of changes in pO_2 and tumor volume within the group, and an unpaired *t* test was used to determine the statistical significance of differences between groups. The paired comparison reduces the animal to animal heterogeneity and eliminates differences of the baseline pO_2. The correlation coefficients between the changes in tumor pO_2 and volume were determined using the statistical package S-Plus 6.1. All data are expressed as means ± SE.

RESULTS

Plasma Concentration of UCN-01

The mice were selected randomly at 24 and 48 h after UCN-01 treatments to determine the plasma concentration of UCN-01. The HPLC results indicated 91 ± 27 n*M* ($n = 4$) and 101 ± 28 n*M*($n = 3$) UCN-01 concentrations at 24 and 48 h, respectively. No significant difference in the plasma concentration of UCN-01 at 24 and 48 h was observed. We did not see any apparent toxicity due to UCN-01 treatments in these mice.

Effect of Radiotherapy and/or UCN-01 on RIF-1 Tumor Oxygenation

The tumor pO_2 measured over 6 consecutive days in the five experimental groups is shown in Fig. 1. No significant difference in the baseline tumor pO_2 between groups was observed. The

tumor pO_2 of the control and UCN-01 alone groups did not change significantly during 5 days of subsequent measurements. However, the tumor pO_2 of the group irradiated with 20 Gy increased significantly on days 3 to 5. The tumor pO_2 on days 4 and 5 after irradiation were significantly higher than the corresponding tumor pO_2 of controls and UCN-01 alone groups. A highly significant increase in tumor pO_2 was observed in the UCN-01/20 Gy group from day 1 onward, and the tumor pO_2 remained at significantly higher levels at around 16–28 mmHg during 5 days of consecutive measurements.

The tissue pO_2 of the 20 Gy/UCN-01 tumors also increased significantly from day 1 compared to baseline pO_2, and the tumor pO_2 remained at 23–30 mmHg during 5 days of consecutive measurements. The increases in tumor pO_2 observed from day 1 in UCN-01/20 Gy and 20 Gy/UCN-01 groups were not significantly different from each other during 5 days of consecutive measurements. However, these tumor pO_2 were significantly higher than the control (day 1–day 5), 20 Gy (day 1–day 4) and UCN-01 (day 1–day 5) groups.

Effect of Radiotherapy and/or UCN-01 on RIF-1 Tumor Growth

The baseline tumor volume and the effect of radiation and/or UCN-01 treatment on tumor growth are shown in Fig. 2. There were no significant differences between the groups in baseline tumor volume. The volumes of the control tumors increased significantly. The treatment with 20 Gy resulted in tumor growth delay, but the tumor volumes observed on days 5 and 6 were significantly higher than the pretreatment tumor volume (day 0). The tumors treated with UCN-01 alone also showed a decline in tumor growth, although the tumor volumes were also significantly higher than the baseline from day 3.

In contrast to the other groups, the tumors treated with UCN-01/20 Gy showed a significant decrease from the pretreatment volume from day 2. The 20 Gy/UCN-01 treatment also resulted in a significant tumor inhibition compared to pretreatment from day 2. Notably, the tumor volumes of the UCN-01/20 Gy and 20 Gy/UCN-01 groups were significantly lower from day 2 compared to all other groups. However, the tumor growth inhibition observed in the UCN-01/20 Gy and 20 Gy/UCN-01 groups were similar during the entire course of measurements.

Correlation between Tumor Oxygenation and Growth

No significant correlation was observed between tumor pO_2 and tumor volume in the control, 20 Gy and UCN-01 alone groups (data not shown). However, a significant correlation between tumor pO_2 and volume measured on day 1 to day 5 was observed in the UCN-01/20 Gy (r average = −0.66, $P = 0$) and 20 Gy/UCN-01 groups (r average= −0.6, $P = 0.002$) (Fig. 3 and Fig. 4).

DISCUSSION

Several pharmacological agents such as hypoxic cell sensitizers and pyrimidine analogues have been investigated in attempts to increase the tumoricidal effects of radiotherapy (3). However, these approaches have shown little success because efficacious levels could not be achieved *in vivo* without undue toxicity. Furthermore, the lack of methods to measure tumor hypoxia directly during these treatments has limited the complete understanding of their effect and optimization. Cell cycle arrest also undermines the therapeutic outcome of modalities such as chemotherapy and radiotherapy. Accordingly, cell cycle checkpoint inhibitors are being investigated in the hope that they will enhance cell killing after DNA damage by preventing cell cycle arrest, thereby driving cells to mitotic catastrophe. An added advantage with inhibitors such as UCN-01 is that extremely low concentrations (10–100 n*M*) could be used to enhance therapeutic outcome (14,15,21,22,25,26). Surprisingly, in spite of its inhibitory

effect on various malignant cells, there have not been attempts to investigate its potential application in a multimodal approach along with external-beam radiotherapy.

The RIF-1 tumors were hypoxic on day 0, and no change in tumor pO_2 was observed in the control and UCN-01 groups. Both UCN-01 and radiation treatments delayed tumor growth, but the growth delay was greater in the group treated with 20 Gy. However, neither treatment decreased tumor volumes. The baseline tumor pO_2 and the increase on days 3 to 5 after irradiation are in agreement with our earlier findings (10). Several different mechanisms have been suggested for reoxygenation after irradiation, such as reduced oxygen consumption, migration of hypoxic cells to an oxygenated state, and improved microcirculation (27–29).

A significant inhibition of tumor growth was observed in tumors treated with UCN-01/20 Gy accompanied by a significant increase in tumor pO_2. The tumors treated with 20 Gy/UCN-01 also had significant growth inhibition and an increase in tumor pO_2. Tumor oxygenation observed with these treatments is likely due to increased tumor cell killing, reduced oxygen consumption, and a decrease in interstitial pressure with tumor shrinkage.

The UCN-01/20 Gy and 20 Gy/UCN-01 groups showed an increase in tumor pO_2 with decreasing tumor volume (Fig. 3 and Fig. 4). Therefore, changes in tumor pO_2 could be used as a potential marker for tumor inhibition. To our knowledge, this is the first report of the changes in tumor pO_2 in a multimodal approach of UCN-01 with radiotherapy. The noteworthy increase in tumor pO_2 from a pretreatment hypoxic level to a well-oxygenated level is likely to have a significant impact in fractionated radiotherapy protocols.

UCN-01 alone affected tumor growth and inhibition irrespective of the sequence of UCN-01 and radiation. This suggests that the effect may not be due to targeting Chk1. UCN-01 is also a non-specific kinase inhibitor that, in addition to Chk1, inhibits other kinases including PKC, PDK1 and C-TAK1 (30,31). UCN-01 was originally developed as a PKC inhibitor. When it was tested in animal models as a single agent, it induced tumor growth delay (32–34). In its combined application with DNA-damaging modalities, the sequence of treatment is important and is related to the p53 status of the tumor. Irradiation of p53 wild-type tumors such as RIF-1 is expected to induce a p53 response that protects the tumor from subsequent Chk1 inhibition. However, if Chk1 is inhibited during the time of DNA damage, the cell killing is enhanced because the p53 response has not been induced (35,36). Irrespective of the underlying mechanism, the tumor inhibition is significant and could be used to induce tumor regression in several malignancies.

In summary, these results provide evidence that UCN-01 in combination with radiotherapy could provide an effective tool for tumor inhibition. Repeated tumor pO_2 measurements using EPR oximetry provide crucial data on tumor pO_2 during this multimodal approach. The observed changes in tumor pO_2 could be used as a marker to predict outcome. The changes in tumor pO_2 also could be used to schedule irradiations at times of increased tumor oxygenation to optimize the outcome of a fractionated regimen. Furthermore, tumor pO_2 could be used to identify responders and non-responders at early times during the treatment, which will allow clinicians to prescribe alternate therapies for non-responders.

Acknowledgments

We thank Drs. Seema Gupta and Julia O'Hara for preliminary experiments. This study was supported by NIH grants CA120919, CA118069, CA117874 and P01EB2180. This work was presented at 54th Annual Meeting of the Radiation Research Society, Boston, MA, September 21–24, 2008.

REFERENCES

1. Gerber DE, Chan TA. Recent advances in radiation therapy. Am. Fam. Physician 2008;78:1254–1262. [PubMed: 19069018]
2. Moeller BJ, Richardson RA, Dewhirst MW. Hypoxia and radiotherapy: opportunities for improved outcomes in cancer treatment. Cancer Metastasis Rev 2007;26:241–248. [PubMed: 17440683]
3. Overgaard J. Hypoxic radiosensitization: adored and ignored. J. Clin. Oncol 2007;25:4066–4074. [PubMed: 17827455]
4. Vaupel P. Hypoxia and aggressive tumor phenotype: implications for therapy and prognosis. Oncologist 2008;13:21–26. [PubMed: 18458121]
5. Brizel DM, Scully SP, Harrelson JM, Layfield LJ, Bean JM, Prosnitz LR, Dewhirst MW. Tumor oxygenation predicts for the likelihood of distant metastases in human soft tissue sarcoma. Cancer Res 1996;56:941–943. [PubMed: 8640781]
6. Swartz HM, Clarkson RB. The measurement of oxygen *in vivo* using EPR techniques. Phys. Med. Biol 1998;43:1957–1975. [PubMed: 9703059]
7. Khan N, Williams BB, Hou H, Li H, Swartz HM. Repetitive tissue pO_2 measurements by electron paramagnetic resonance oximetry: current status and future potential for experimental and clinical studies. Antioxid. Redox Signal 2007;9:1169–1182. [PubMed: 17536960]
8. O'Hara JA, Goda F, Demidenko E, Swartz HM. Effect on regrowth delay in a murine tumor of scheduling split-dose irradiation based on direct pO_2 measurements by electron paramagnetic resonance oximetry. Radiat. Res 1998;150:549–556. [PubMed: 9806597]
9. Hou H, Khan N, Grinberg OY, Yu H, Grinberg SA, Lu S, Demidenko E, Steffen RP, Swartz HM. The effects of Efaproxyn (efaproxiral) on subcutaneous RIF-1 tumor oxygenation and enhancement of radiotherapy-mediated inhibition of tumor growth in mice. Radiat. Res 2007;168:218–225. [PubMed: 17638413]
10. Hou H, Lariviere JP, Demidenko E, Gladstone D, Swartz H, Khan N. Repeated tumor pO_2 measurements by multi-site EPR oximetry as a prognostic marker for enhanced therapeutic efficacy of fractionated radiotherapy. Radiother. Oncol 2009;91:126–131. [PubMed: 19013657]
11. Hou H, Khan N, O'Hara JA, Grinberg OY, Dunn JF, Abajian MA, Wilmot CM, Makki M, Demidenko E, Swartz HM. Effect of RSR13, an allosteric hemoglobin modifier, on oxygenation in murine tumors: an *in vivo* electron paramagnetic resonance oximetry and bold MRI study. Int. J. Radiat. Oncol. Biol. Phys 2004;59:834–843. [PubMed: 15183487]
12. Khan N, Li H, Hou H, Lariviere JP, Gladstone DJ, Demidenko E, Swartz HM. Tissue pO_2 of orthotopic 9L and C6 gliomas and tumor-specific response to radiotherapy and hyperoxygenation. Int. J. Radiat. Oncol. Biol. Phys 2009;73:878–885. [PubMed: 19136221]
13. Swartz HM, Khan N, Buckey J, Comi R, Gould L, Grinberg O, Hartford A, Hopf H, Hou H, Walczak T. Clinical applications of EPR: overview and perspectives. NMR Biomed 2004;17:335–351. [PubMed: 15366033]
14. Eastman A. Cell cycle checkpoints and their impact on anticancer therapeutic strategies. J. Cell Biochem 2004;91:223–231. [PubMed: 14743382]
15. Bunch RT, Eastman A. Enhancement of cisplatin-induced cytotoxicity by 7-hydroxystaurosporine (UCN-01), a new G_2-checkpoint inhibitor. Clin. Cancer Res 1996;2:791–797. [PubMed: 9816232]
16. Levesque AA, Kohn EA, Bresnick E, Eastman A. Distinct roles for p53 transactivation and repression in preventing UCN-01-mediated abrogation of DNA damage-induced arrest at S and G_2 cell cycle checkpoints. Oncogene 2005;24:3786–3796. [PubMed: 15782134]
17. Perez RP, Lewis LD, Beelen AP, Olszanski AJ, Johnston N, Rhodes CH, Beaulieu B, Ernstoff MS, Eastman A. Modulation of cell cycle progression in human tumors: a pharmacokinetic and tumor molecular pharmacodynamic study of cisplatin plus the Chk1 inhibitor UCN-01 (NSC 638850). Clin. Cancer Res 2006;12:7079–7085. [PubMed: 17145831]
18. Welch S, Hirte HW, Carey MS, Hotte SJ, Tsao MS, Brown S, Pond GR, Dancey JE, Oza AM. UCN-01 in combination with topotecan in patients with advanced recurrent ovarian cancer: a study of the Princess Margaret Hospital Phase II consortium. Gynecol. Oncol 2007;106:305–310. [PubMed: 17537491]

19. Edelman MJ, Bauer KS Jr, Wu S, Smith R, Bisacia S, Dancey J. Phase I and pharmacokinetic study of 7-hydroxystaurosporine and carboplatin in advanced solid tumors. Clin. Cancer Res 2007;13:2667–2674. [PubMed: 17473198]
20. Jimeno A, Rudek MA, Purcell T, Laheru DA, Messersmith WA, Dancey J, Carducci MA, Baker SD, Hidalgo M, Donehower RC. Phase I and pharmacokinetic study of UCN-01 in combination with irinotecan in patients with solid tumors. Cancer Chemother. Pharmacol 2008;61:423–433. [PubMed: 17429623]
21. Meng QH, Zhou LX, Luo JL, Cao JP, Tong J, Fan SJ. Effect of 7-hydroxystaurosporine on glioblastoma cell invasion and migration. Acta Pharmacol. Sin 2005;26:492–499. [PubMed: 15780200]
22. Tsuchida E, Urano M. The effect of UCN-01 (7-hydroxystaurosporine), a potent inhibitor of protein kinase C, on fractionated radiotherapy or daily chemotherapy of a murine fibrosarcoma. Int. J. Radiat. Oncol. Biol. Phys 1997;39:1153–1161. [PubMed: 9392558]
23. Hou H, Lariviere JP, Demidenko E, Gladstone D, Swartz H, Khan N. Repeated tumor pO_2 measurements by multi-site EPR oximetry as a prognostic marker for enhanced therapeutic efficacy of fractionated radiotherapy. Radiother. Oncol 2009;91:126–131. [PubMed: 19013657]
24. Gallez B, Swartz HM. *In vivo* EPR: when, how and why? NMR Biomed 2004;17:223–225. [PubMed: 15366024]
25. Rini BI, Weinberg V, Shaw V, Scott J, Bok R, Park JW, Small EJ. Time to disease progression to evaluate a novel protein kinase C inhibitor, UCN-01, in renal cell carcinoma. Cancer 2004;101:90–95. [PubMed: 15221993]
26. Shao RG, Cao CX, Shimizu T, O'Connor PM, Kohn KW, Pommier Y. Abrogation of an S-phase checkpoint and potentiation of camptothecin cytotoxicity by 7-hydroxystaurosporine (UCN-01) in human cancer cell lines, possibly influenced by p53 function. Cancer Res 1997;57:4029–4035. [PubMed: 9307289]
27. Brown JM. Evidence for acutely hypoxic cells in mouse tumours, and a possible mechanism of reoxygenation. Br. J. Radiol 1979;52:650–656. [PubMed: 486895]
28. Kallman RF. The phenomenon of reoxygenation and its implications for fractionated radiotherapy. Radiology 1972;105:135–142. [PubMed: 4506641]
29. Zhao D, Constantinescu A, Chang CH, Hahn EW, Mason RP. Correlation of tumor oxygen dynamics with radiation response of the dunning prostate R3327-HI tumor. Radiat. Res 2003;159:621–631. [PubMed: 12710873]
30. Busby EC, Leistritz DF, Abraham RT, Karnitz LM, Sarkaria JN. The radiosensitizing agent 7-hydroxystaurosporine (UCN-01) inhibits the DNA damage checkpoint kinase hChk1. Cancer Res 2000;60:2108–2112. [PubMed: 10786669]
31. Davies SP, Reddy H, Caivano M, Cohen P. Specificity and mechanism of action of some commonly used protein kinase inhibitors. Biochem. J 2000;351:95–105. [PubMed: 10998351]
32. Akinaga S, Gomi K, Morimoto M, Tamaoki T, Okabe M. Antitumor activity of UCN-01, a selective inhibitor of protein kinase C, in murine and human tumor models. Cancer Res 1991;51:4888–4892. [PubMed: 1893379]
33. Mizuno K, Noda K, Ueda Y, Hanaki H, Saido TC, Ikuta T, Kuroki T, Tamaoki T, Hirai S, Ohno S. UCN-01, an anti-tumor drug, is a selective inhibitor of the conventional PKC subfamily. FEBS Lett 1995;359:259–261. [PubMed: 7867810]
34. Pollack IF, Kawecki S, Lazo JS. Blocking of glioma proliferation *in vitro* and *in vivo* and potentiating the effects of BCNU and cisplatin: UCN-01, a selective protein kinase C inhibitor. J. Neurosurg 1996;84:1024–1032. [PubMed: 8847567]
35. Levesque AA, Fanous AA, Poh A, Eastman A. Defective p53 signaling in p53 wild-type tumors attenuates p21waf1 induction and cyclin B repression rendering them sensitive to Chk1 inhibitors that abrogate DNA damage-induced S and G_2 arrest. Mol. Cancer Ther 2008;7:252–262. [PubMed: 18281511]
36. Levesque AA, Eastman A. p53-based cancer therapies: Is defective p53 the Achilles heel of the tumor? Carcinogenesis 2007;28:13–20. [PubMed: 17088261]

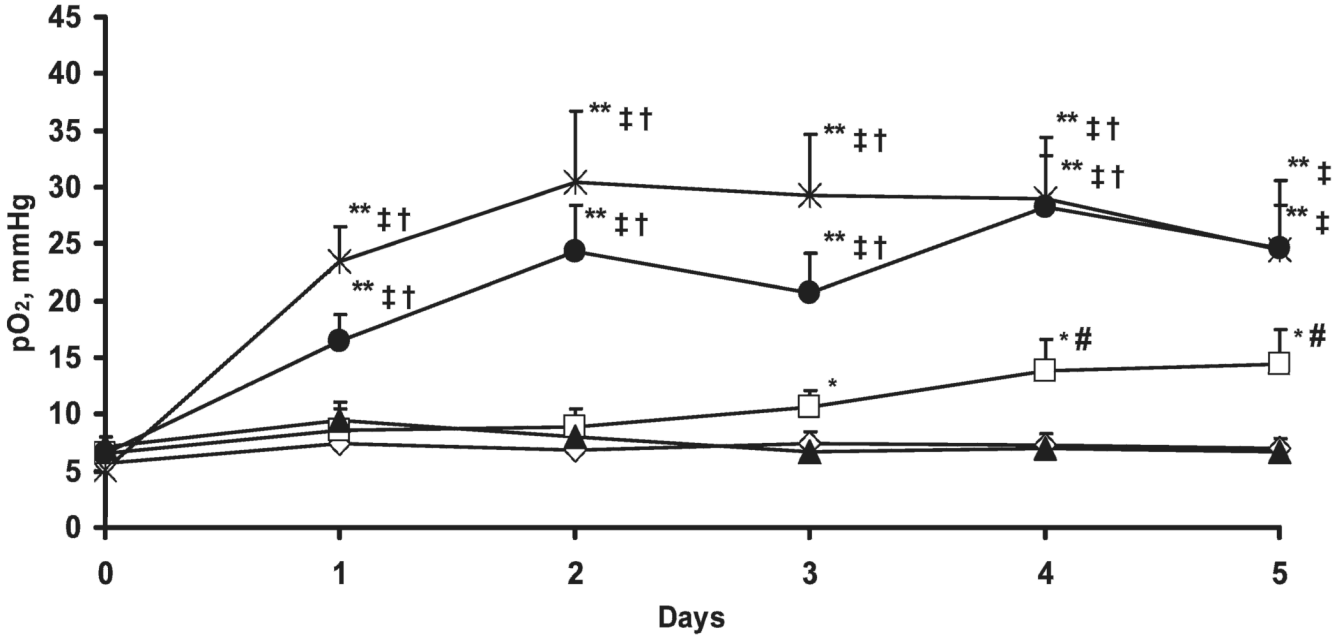

FIG. 1.

pO_2 in RIF-1 tumors in the control (◊), 20 Gy (□), UCN-01 (▲), UCN-01/20 Gy (●), $n = 8$, and 20 Gy/UCN-01 (✳) groups. The tumor pO_2 is expressed as mean + SE. $^{*}P < 0.05$ compared with baseline pO_2 (day 0); $^{**}P < 0.01$ compared with baseline pO_2 (day 0); $^{\#}P < 0.05$ compared with control and UCN-01 alone groups; $^{\ddagger}P < 0.01$ compared with control and UCN-01 alone groups; $^{\dagger}P < 0.01$ compared with 20 Gy group.

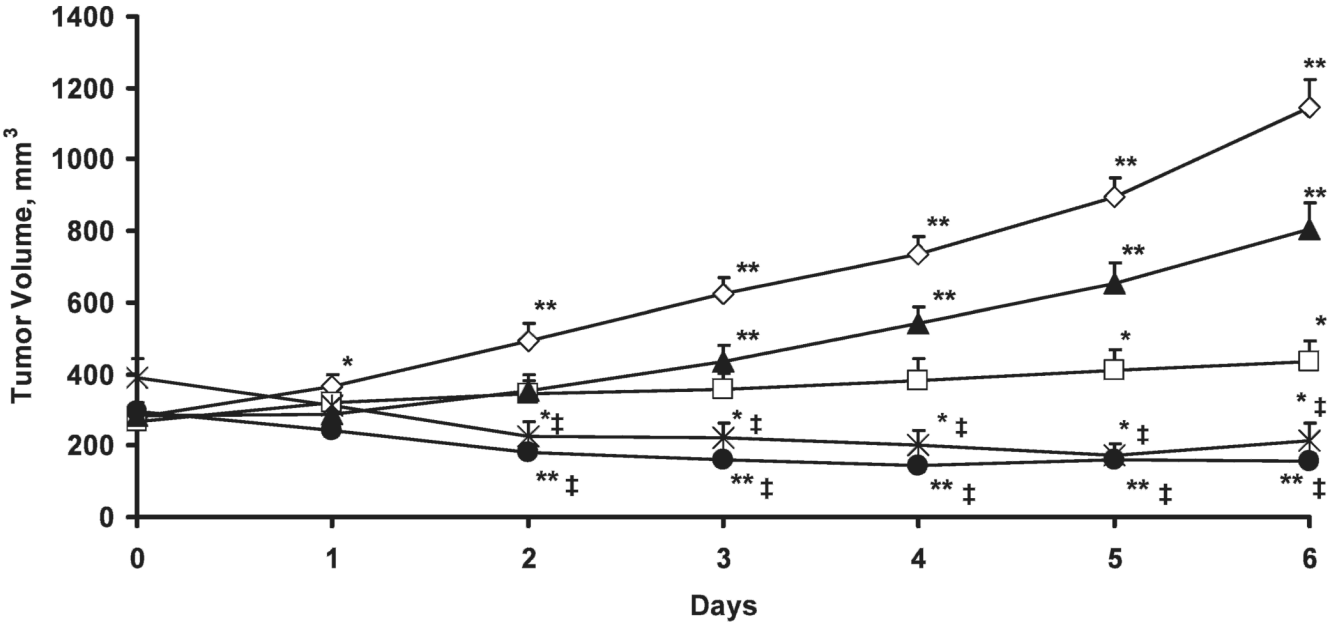

FIG. 2.

Volume of RIF-1 tumors in the control (◊), 20 Gy (□), UCN-01 (▲), and UCN-01/20 Gy (●), and 20 Gy/UCN-01 (✳) groups. The tumor volume is expressed as mean + SE. **P* < 0.05 and ***P* < 0.01 compared with baseline tumor volume (day 0); ‡*P* < 0.01 compared with control, UCN-01 alone and 20 Gy groups.

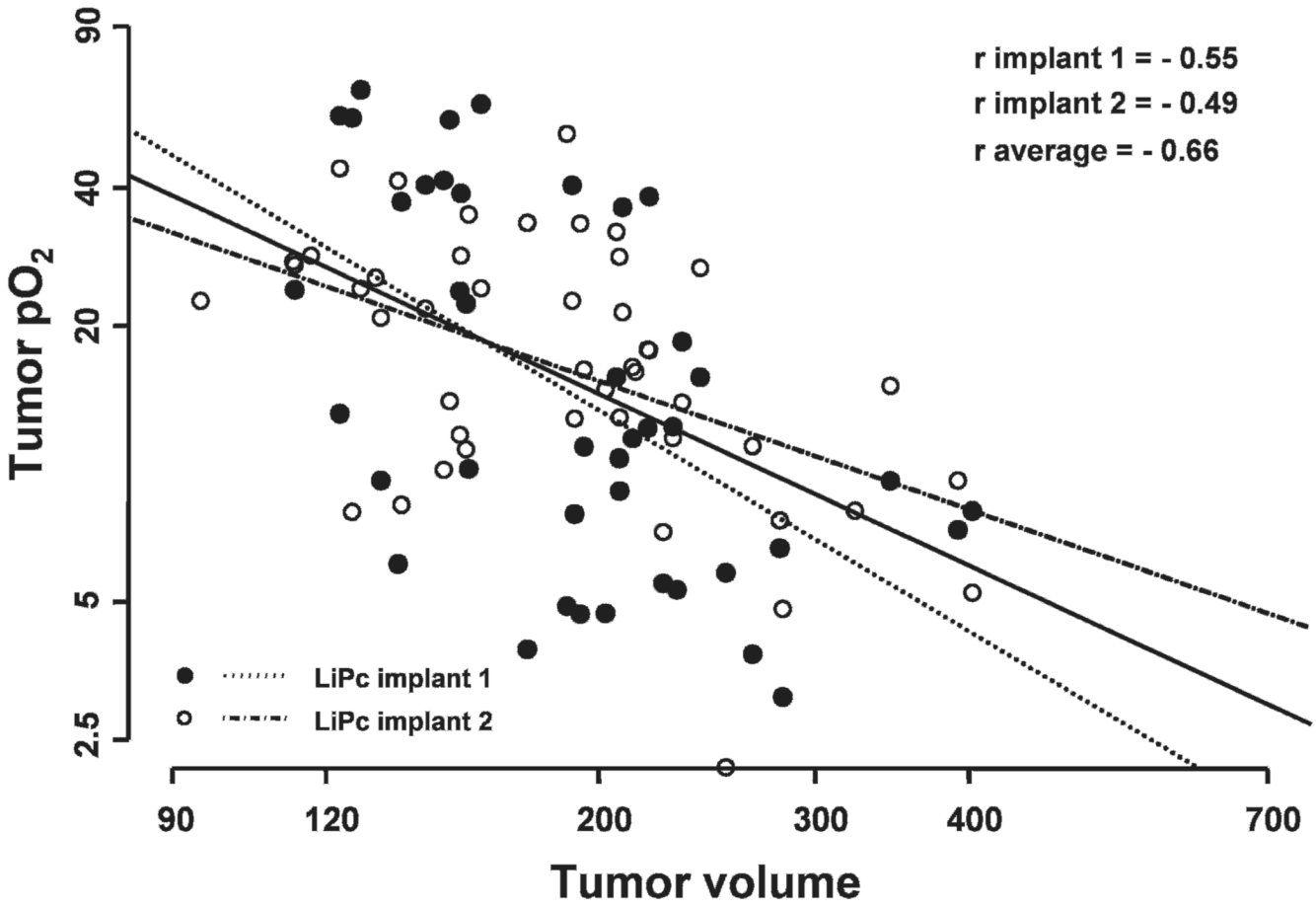

FIG. 3.

Correlation between the tumor pO_2 measured from the two LiPc implants of each tumor and tumor volume on day 1 to day 5 in UCN-01/20 Gy group. An inverse correlation indicates an increase in tumor pO_2 with decreased tumor volume.

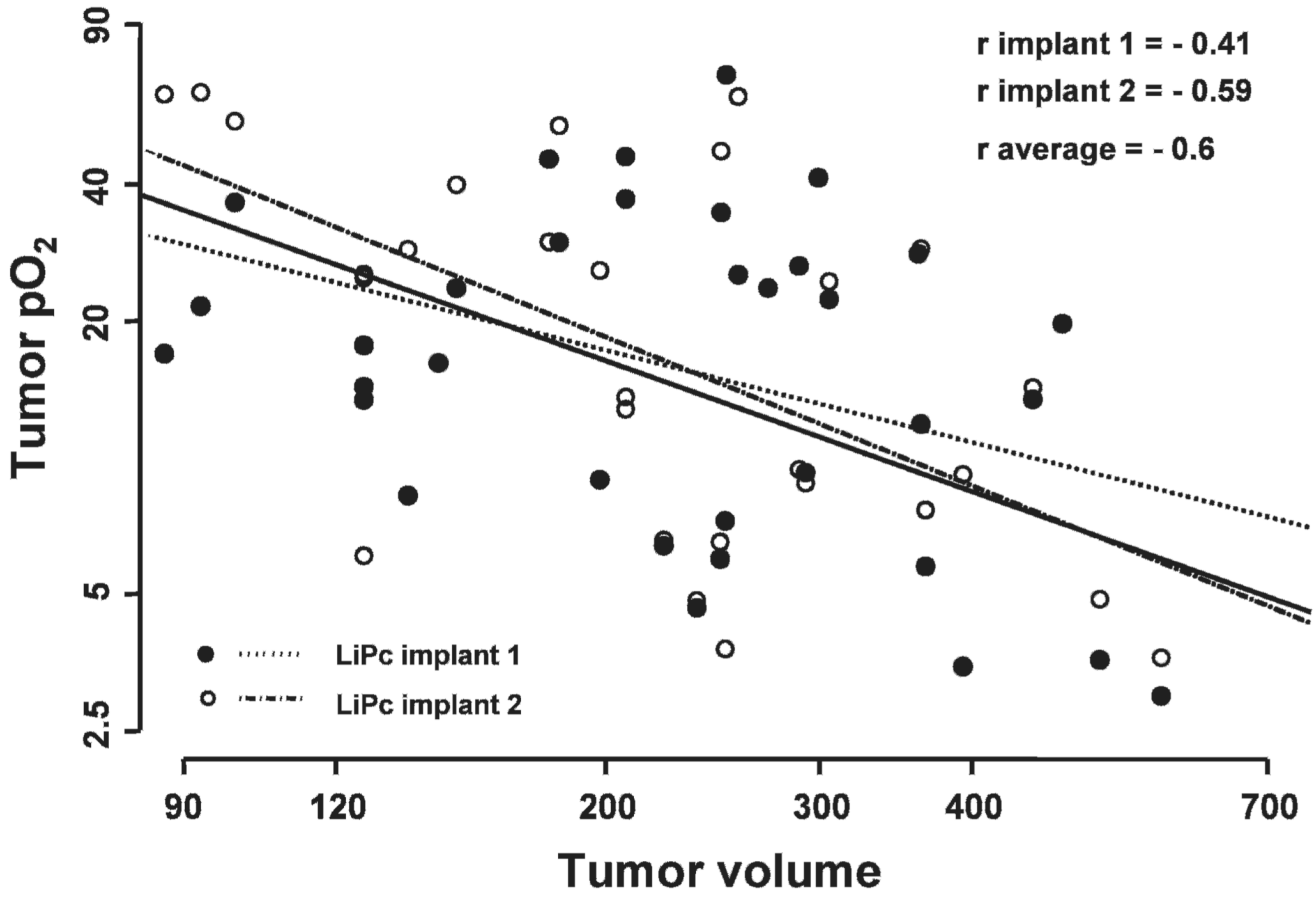

FIG. 4.

Correlation between the tumor pO_2 measured from the two LiPc implants of each tumor and tumor volume on day 1 to day 5 in the 20 Gy/UCN-01 group. An inverse correlation indicates an increase in tumor pO_2 with decreased tumor volume.